some experiments, the bias voltage was increased with a concurrent decrease in the stabilization current in order to maintain a constant electric field. Dissociation was observed only at high bias voltages. If the STM tip is brought into mechanical contact with the adsorbed molecule, then fragmentation can occur. We think that this process essentially involves severe local stress. However, under our typical conditions for recording images (+2 V bias, 200 pA), mechanical tip-molecule interactions are negligible, as evidenced by stable, reproducible images from scan to scan. Also, the tip retracts away from the surface as the voltage is increased from the normal scanning bias. Thus, we can rule out mechanical interactions with the tip as a dissociation mechanism during the scans at increased bias voltages. The evidence suggests that the observed dissociation processes are a direct consequence of the high flux of low-energy electrons incident on the adsorbed molecules.

REFERENCES AND NOTES

1. R. S. Becker, J. A. Golovchenko, B. S. Swartzentruber, *Nature* **325**, 419 (1987).
2. J. S. Foster *et al.*, *ibid.* **331**, 324 (1988).
3. D. M. Eigler and E. K. Schweizer, *ibid.* **344**, 524 (1990).
4. J. A. Stroscio and D. M. Eigler, *Science* **254**, 1319 (1991).
5. D. M. Eigler, C. P. Lutz, W. E. Rudge, *Nature* **352**, 600 (1991).
6. I.-W. Lyo and Ph. Avouris, *Science* **253**, 173 (1991).
7. See reports from STM 89 [*J. Vac. Sci. Technol. A* **8** (1990)] and STM 90 [*ibid.* **9** (1991)].
8. C. F. Quate, in *Proceedings of the NATO Science Forum '90*, L. Esaki, Ed. (Plenum, New York, in press).
9. R. S. Becker, G. S. Higashi, Y. J. Chabal, A. J. Becker, *Phys. Rev. Lett.* **65**, 1917 (1990).
10. C. R. K. Marrian, E. A. Dobisz, R. J. Colton, *J. Vac. Sci. Technol. A* **8**, 3563 (1990).
11. G. T. Furukawa and R. P. Park, *J. Res. Natl. Bur. Std.* **55**, 255 (1955).
12. Y. G. Kim, P. A. Dowben, J. T. Spencer, G. O. Ramseyer, *J. Vac. Sci. Technol. A* **7**, 2796 (1989).
13. Ph. Avouris, I.-W. Lyo, F. Bozso, E. Kaxiras, *ibid.* **8**, 3405 (1990).
14. Ph. Avouris, *J. Phys. Chem.* **94**, 2246 (1990).
15. R. A. Rosenberg *et al.*, *Appl. Phys. Lett.* **58**, 607 (1991).
16. F. K. Perkins, R. A. Rosenberg, S. Lee, P. A. Dowben, *J. Appl. Phys.* **69**, 4103 (1991).
17. Ph. Avouris and R. Wolkow, *Phys. Rev. B* **39**, 509 (1989).
18. J. Tersoff and D. R. Hamann, *ibid.* **31**, 805 (1985).
19. T. Klitsner *et al.*, *ibid.* **41**, 3837 (1990).
20. N. D. Lang, *ibid.* **34**, 5947 (1986).
21. See L. A. Laws, R. M. Stevens, W. N. Lipscomb, *J. Am. Chem. Soc.* **94**, 4467 (1972).
22. S. G. Shore, in *Boron Hydride Chemistry*, E. L. Muetterties, Ed. (Academic Press, New York, 1975), chap. 3.
23. A clean tip, that is, one that does not deposit material onto the sample surface when the bias voltage is increased, is essential. The tip had to be cleaned by electron bombardment at ~10 nA and −10 V for a few minutes prior to imaging $B_{10}H_{14}$ molecules.
24. L. J. Whitman, J. A. Stroscio, R. A. Dragoset, R. J. Celotta, *Science* **251**, 1206 (1991).
25. In interpreting topographic images of the dissociation products, one should keep in mind that these reflect a combination of geometric and electronic structures.
26. A. Quayle, *J. Appl. Chem. (London)* **9**, 395 (1959).
27. T. T. Tsong, *Atom-Probe Field Ion Microscopy* (Cambridge Univ. Press, Cambridge, 1990).

28. We thank P. Dowben of Syracuse University for providing high-purity samples of $B_{10}H_{14}$ and I.-W. Lyo for invaluable technical help.

29 October 1991; accepted 7 January 1992

C_{60} Rotation in the Solid State: Dynamics of a Faceted Spherical Top

ROBERT D. JOHNSON,* COSTANTINO S. YANNONI, HARRY C. DORN,† JESSE R. SALEM, DONALD S. BETHUNE

The rotational dynamics of C_{60} in the solid state have been investigated with carbon-13 nuclear magnetic resonance (^{13}C NMR). The relaxation rate due to chemical shift anisotropy ($1/9T_1^{CSA}$) was precisely measured from the magnetic field dependence of T_1, allowing the molecular reorientational correlation time, τ, to be determined. At 283 kelvin, τ = 9.1 picoseconds; with the assumption of diffusional reorientation this implies a rotational diffusion constant $D = 1.8 \times 10^{10}$ per second. This reorientation time is only three times as long as the calculated τ for free rotation and is shorter than the value measured for C_{60} in solution (15.5 picoseconds). Below 260 kelvin a second phase with a much longer reorientation time was observed, consistent with recent reports of an orientational phase transition in solid C_{60}. In both phases τ showed Arrhenius behavior, with apparent activation energies of 1.4 and 4.2 kilocalories per mole for the high-temperature (rotator) and low-temperature (ratchet) phases, respectively. The results parallel those found for adamantane.

THE FACT THAT C_{60} MOLECULES IN the solid state interact only weakly leads to interesting dynamical behavior. Rotational dynamics of molecules in condensed phases can be probed with NMR spectroscopy. In earlier NMR studies of solid C_{60} (*1, 2*), it was found that the spectrum at ambient temperature consists of a relatively narrow line rather than a broad powder pattern, as expected for randomly oriented stationary molecules. This sharp spectrum implies rapid isotropic molecular reorientation. Powder patterns reflect the variation in the magnetic shielding of a nucleus with molecular orientation (chemical shift anisotropy or CSA). Below 100 K the reorientation rate slows sufficiently to allow determination of the chemical shift tensor elements from the shape of the NMR line (*1*).

The molecular reorientation time τ can be found from measurements of the spin lattice relaxation time, T_1, because for rotating molecules, anisotropic shielding leads to fluctuating fields proportional to the external magnetic field (B_0), with a concomitant relaxation rate proportional to B_0^2. The CSA relaxation mechanism is expected to dominate in both liquids and solids at sufficiently high fields. A classic T_1 minimum was observed at 233 K in the first relaxation measurements on solid C_{60}. Interpreting this in terms of CSA relaxation yielded a value of τ = 2.1 ns at this temperature (*1*).

More recently, Heiney *et al.* (*3*) found from x-ray studies and calorimetry that solid C_{60} exhibits a phase transition near 249 K from a simple cubic structure at low temperatures to a face-centered-cubic (FCC) structure. This transition was examined with NMR by Tycko *et al.* (*4*), who found a break in the T_1 relaxation rate at 260 K. These studies suggest that the phase above the transition temperature is characterized by free rotation or rotational diffusion and that the phase below the transition is characterized by jump rotational diffusion between symmetry-equivalent orientations.

In this report we present detailed measurements of the reorientational correlation time τ for solid C_{60} over the temperature range 240 to 331 K. The quantity τ was calculated from the CSA relaxation rate and the measured chemical shift tensor elements. Because the CSA relaxation rate has a unique quadratic dependence on magnetic field, measurement of T_1 as a function of magnetic field allows the CSA contribution to be obtained and separated from non-CSA (NCSA) relaxation mechanisms. Results were obtained both above and below the phase transition, which we found at 260 K

IBM Research Division, Almaden Research Center, 650 Harry Road, San Jose, CA 95120–6099.

*To whom correspondence should be addressed.
†Permanent address: Department of Chemistry, Virginia Polytechnic Institute and State University, Blacksburg, VA 24061.

from both NMR and calorimetry. The low-temperature ratchet phase was characterized by a much faster relaxation rate and by reorientational correlation times that were ~30 times as long as that for the high-temperature rotator phase at temperatures near the phase transition. The temperature dependence of τ for both phases can be described by Arrhenius expressions, and activation energies for reorientation were obtained.

A sample of isotopically enriched soot (~9% ^{13}C) was prepared as described (*5, 6*). Fullerenes were extracted from the ^{13}C-labeled soot with toluene and purified by liquid chromatography (7). The purified C_{60} was continuously extracted for 3 hours with supercritical CO_2 (70°C) to remove solvent, heated to 200°C under vacuum for 1 hour to remove absorbed CO_2, and sealed in an NMR tube 5 mm in diameter. NMR experiments were carried out at ^{13}C NMR frequencies of 125.7, 75.4, 62.9, and 50.3 MHz (11.74, 7.06, 5.87, and 4.71 T, respectively).

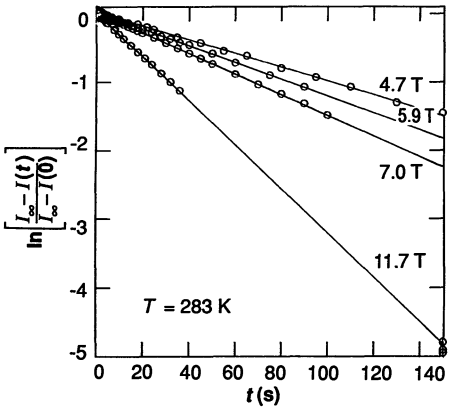

Fig. 1. Plot of $\ln\{[I_\infty - I(t)]/[I_\infty - I(0)]\} = -t/T_1$ versus delay time t for inversion-recovery experiments on the C_{60} sample at magnetic field strengths of 11.74, 7.06, 5.87, and 4.71 T at 283 K. $I(0)$ and I_∞ are signals measured at $t = 0$ and $t > 5T_1$.

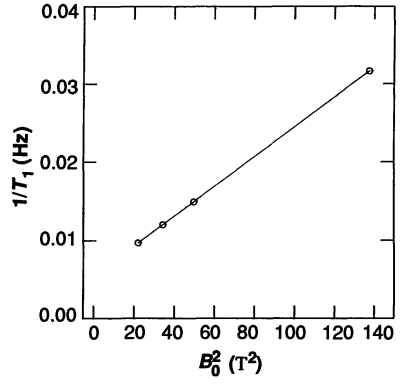

Fig. 2. Plot of relaxation rate $1/T_1$ versus the square of the magnetic field for the experiments in Fig. 1.

The T_1 rates for this sample were measured with the inversion-recovery technique (*8*). The results obtained for the signal recovery at 283 K for all four fields are shown in Fig. 1. For each field the recovery of magnetization can be described by a simple exponential function; the recovery times (T_1's) are strongly field-dependent.

In general the T_1 rate includes both CSA and non-CSA contributions: $(1/T_1) = (1/T_1^{CSA} + 1/T_1^{NCSA})$. If one assumes that the reorientation of the molecules can be described as isotropic rotational diffusion, the CSA relaxation rate can be written in the form (*9, 10*)

$$\frac{1}{T_1^{CSA}} = \gamma^2 B_0^2 \left[\frac{2}{3} A^2 \frac{\tau_A}{(1 + \omega^2 \tau_A^2)} + \frac{2}{15} S^2 \frac{\tau_S}{(1 + \omega^2 \tau_S^2)} \right] \quad (1)$$

where $\gamma = 67.31 \times 10^6$ rad s^{-1} T^{-1} (the ^{13}C magnetogyric ratio), τ_A and τ_S are rotational correlation times, and $\omega = \gamma B_0$ is the angular Larmor frequency. The factors S^2 and A^2 arise from the symmetric and antisymmetric components [$\sigma^S \equiv (\sigma + \sigma^T)/2$ and $\sigma^A \equiv (\sigma - \sigma^T)/2$] of the shielding tensor σ (where σ^T is the transpose of σ). The reorientational correlation times are related to the rotational diffusion constant D by $1/6D \equiv \tau = \tau_S = \tau_A/3$ (*11*). For isotropic rotational diffusion, the mean-square angle of rotation in a time Δt about each axis is given by $\langle\theta_i^2\rangle = 2D\Delta t$. In the limit of short correlation times ($\omega\tau \ll 1$), the expression on the right side of Eq. 1 shows the signature B_0^2 dependence of the CSA contribution to the T_1 rate noted above.

In Fig. 2, the T_1 rates obtained from fits to the data in Fig. 1 are plotted against B_0^2. The dependence is linear to a high degree of accuracy, with a slope of 0.191 ± 0.003 mHz T^{-2} and an intercept $1/T_1^{NCSA} = 5.4$ ± 0.2 mHz. Although the CSA mechanism accounts for most of the relaxation rate at high magnetic field strengths, there is a significant NCSA contribution (37% of the total rate at 7 T, for example). From this data, the reorientational correlation time τ can be obtained from Eq. 1 if the quantities S and A are known. S is defined in terms of the three principal values σ_{11}, σ_{22}, and σ_{33} of the shielding tensor σ^S, known from experiment to be 180, 25, and 220 ppm, respectively (*1, 12*). A value $S^2 = 3.17 \times 10^{-8}$ is found (*13*). A depends on the antisymmetric part of the shielding tensor and is extremely difficult to measure experimentally (*10*). It can be estimated (*14*) that $A^2 \approx 1.4 \pm 1.4 \times 10^{-10}$, so the anisotropic contribution to $1/T_1^{CSA}$ should be relatively small (~6%). With these values for S^2 and A^2, we calculate $\tau = 9.1 \pm 2$ ps at 283 K, yielding a rotational diffusion constant $D = 1.8 \pm 0.4 \times 10^{10}$ s^{-1}.

Examination of the relaxation behavior of solid C_{60} as a function of temperature shows a dramatic effect due to the phase transition. Below 260 K the inversion-recovery data show a biexponential decay: in addition to a component that smoothly continues the τ versus temperature curve measured for the rotator phase at higher temperatures, a second component with a much faster relaxation rate appears (*4*). Figure 3 shows a typical two-component decay, obtained at a temperature $T = 254$ K at 7.06 T, from which two values of T_1 (50 and 1.6 s) can be extracted. The large difference between these two times allows them to be cleanly separated. The fraction of the material in the long T_1 rotator phase was 74% at 254 K and 25% at 241 K. Biexponential behavior was also seen in a sample of C_{60} with 15% C_{70} over a wide range of temperatures, but a highly crystalline C_{60} sample showed biphasic behavior over a range of only 1 K (*15*). Although the relative populations and the exact transition temperatures were sample-dependent, for all samples examined the transition temperatures indicated by NMR and by differential scanning calorimetry (DSC) were in good agreement.

By measuring both T_1 rates at several fields, we obtained reorientational correlation times for both phases using Eq. 1. Although there is clear evidence that the reorientational motion for the ratchet phase cannot be described as isotropic diffusion

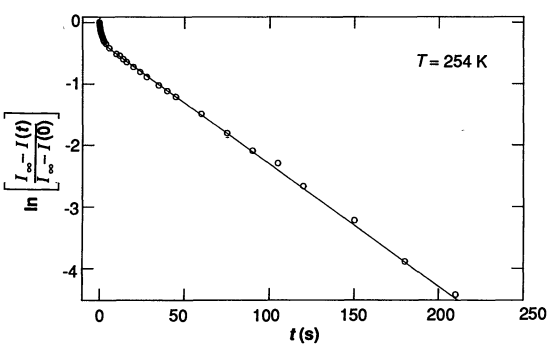

Fig. 3. Log plot of intensity data from an inversion-recovery experiment at 254 K at 7.04 T on the C_{60} sample. A two-component fit to the data yielded T_1 of 1.6 (26%) and 50.0 s (74%), with composition in parentheses.

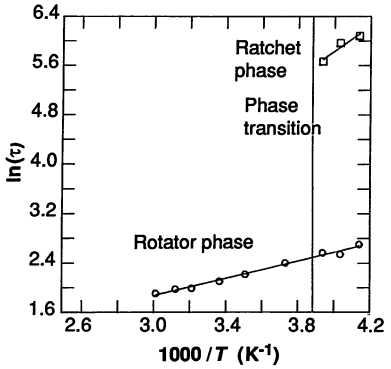

Fig. 4. Arrhenius plot of ln(τ) versus 1000/T for the ratchet and rotator phases, with apparent activation energies of 4.2 and 1.4 kcal mol^{-1} K^{-1}, respectively. Units of τ are picoseconds.

(*3*), we expect that Eq. 1 gives an effective correlation time τ for random jumps between equivalent orientations that retains its physical significance as the time required for molecular motion through an angle of ~1 rad (*9*).

Figure 4 shows the dependence of ln(τ) on 1000/T for both phases. For the high-temperature rotator phase (lower set of points), measurements were made in the temperature range 241 to 331 K, both above and below the phase transition (indicated by the vertical line). Over this temperature range, τ varies from 14.9 to 6.8 ps. Over the same temperature range the NCSA contributions to the T_1 rates are approximately constant, with $1/T_1^{NCSA} \approx 5 \pm 0.5 \times 10^{-3}$ s^{-1}. Possible contributions to the NCSA rate include inter- and intramolecular ^{13}C dipolar relaxation and effects due to trace paramagnetic species. Below the transition the much faster CSA relaxation rates found for the ratchet phase correspond (through Eq. 1) to much longer reorientational correlation times. For this phase, τ varies from 0.44 to 0.29 ns as the temperature varies between 241 and 254 K.

Despite the phase transition, the rotator phase data can be fit very well by a straight line over the entire temperature range, allowing τ for this phase to be described by a single Arrhenius expression: $\tau = \tau_0 \exp(T_a/T)$. The preexponential τ_0 obtained from fitting the data is $\tau_0^{Rot} = 8.1 \pm 1.0 \times 10^{-13}$ s, and the corresponding activation temperature (T_a^{Rot}) is 695 ± 45 K (rotator activation energy $E_a^{Rot} = 1.4 \pm 0.1$ kcal mol^{-1}). This implies that the temperature dependence of the diffusion constant is given by $D = D_0 \exp(-T_a^{Rot}/T)$, with $D_0 = 2.06 \times 10^{11}$ s^{-1}. A similar fit to the data for the ratchet phase (upper part of Fig. 4) yields $\tau_0^{Rat} = 8 \times 10^{-(14\pm1)}$ s and $T_a^{Rat} = 2100 \pm 600$ K ($E_a^{Rat} = 4.2 \pm 1.2$ kcal mol^{-1}). Thus, the activation energy for the ratchet phase is about three times as large as that for the rotator phase. Preliminary measurements on more highly crystalline samples indicate that E_a for the rotator phase is not highly sample-dependent, whereas E_a for the ratchet phase is greater for more perfect crystals (*15*).

Above the phase transition the rotational correlation times for solid C_{60} are remarkably short and in fact are comparable to those for small molecules in solution. For example, a value of τ = 7.2 ps has been measured for tetrachlorocyclopropene in toluene-d_8 at room temperature (*10*). The activation energy and preexponential factors derived for this system ($E_a \approx 1.5$ kcal mol^{-1} near 0°C, and $\tau_0 = 0.65$ ps) are both similar to the values found here for the rotator phase of C_{60}. Surprisingly, similar experiments performed on C_{60} dissolved in tetrachloroethane revealed τ = 15.5 ps at 283 K, showing that C_{60} can reorient faster in the solid than in solution.

The rotational correlation time for the solid can also be compared to the correlation time expected for free molecular rotation, the natural limit for reorientation at high temperature or in the absence of frictional interactions. The ball diameter of 7.1 Å, derived from the C_{60} bond lengths (1.40 and 1.45 Å) (*16–19*), implies a moment of inertia $I = 1.0 \times 10^{-43}$ kg m^2 for C_{60}. For free gas molecules at temperature T, the characteristic time for rotation through 1 rad is $\tau_{FR} \equiv 3/5(I/kT)^{1/2}$ (*20*) (k = Boltzmann constant). At 283 K, τ_{FR} for C_{60} is 3.1 ps. Thus, τ for the molecules in the solid at this temperature is only three times as long as the correlation time expected for unhindered gas-phase rotation. Steele and co-workers (*21*) have pointed out that inertial effects will be significant for values of $\chi \equiv \tau/\tau_{FR} \lesssim 2$. At the highest temperature used in this study (331 K), χ equaled 2.4, a value that is still consistent with a diffusional model (*9, 20*) but near the boundary of the inertial regime. Coherent quasielastic neutron scattering has recently been used to investigate the character of the rotational dynamics of C_{60} (*22*), and a rotational diffusion constant $D_R = 1.4 \times 10^{10}$ s^{-1} at 260 K was deduced. This is in striking agreement with the value 1.42×10^{10} s^{-1} we obtain for 260 K using our values for τ_0^{Rot} and T_a^{Rot}. Additional scattering data at 520 K were used to estimate an activation temperature of ~400 K, which is significantly lower than that found here, possibly because at such a high temperature inertial effects are important, leading to longer values of τ and non-Arrhenius behavior (*21*). A recent molecular dynamics calculation (*23*) yielded, at 283 K, τ = 0.18 ps and a rotational barrier of 300 K. Both of these values are significantly lower than our measured values, but the calculation does show diffusive motion at high temperatures and an orientational ordering transition at ~200 K, in qualitative agreement with experiment.

A structure for the ratchet phase of solid C_{60} has recently been proposed on the basis of neutron diffraction measurements (*19*); this structure simultaneously optimizes the intermolecular interaction between each molecule and its 12 nearest neighbors. Although the detailed nature of motion in this phase is unknown, a simple model can be used to estimate the rate at which the molecules jump between equivalent orientations. A molecule is assumed to turn by an angle $\Delta\Theta = 2\pi/5$ at a time at an average jump rate ν about a fivefold axis axis randomly chosen for each step. This assumption leads to a random walk in the three-dimensional orientation space with a rotational correlation time $\tau = 1/\nu\Delta\Theta^2$ (*24*). The observed τ_{Rat} of 0.29 ns at 254 K then implies a jump rate $\nu = 2.2 \times 10^9$ s^{-1}. Using the values obtained for E_a^{Rat} and τ_0^{Rat}, one predicts a T_1 minimum at 206 K for a 7.06-T field and a correlation time of 3 ms at 86 K. These temperatures are in reasonable accord with the reported T_1 minimum temperature of 233 K at 7 T and the temperature at which a powder pattern due to CSA fully develops at a field of 1.4 T (*1*).

Our results can be compared to the NMR data obtained by Tycko *et al.* (*2*), who obtained activation energies of ~1 and 5 kcal mol^{-1} for the rotator and ratchet phases from the temperature dependence of T_1 measured at a single field. These values are in reasonable agreement with those derived from the data presented here. Our correlation times are shorter than those estimated by Tycko *et al.* (*2*). For the rotator phase at 300 K, Tycko estimated $\tau_c = 12$ ps and our data give τ = 8 ps. Some of this discrepancy may result from our explicitly accounting for non-CSA relaxation, leading to lower CSA relaxation rates and shorter correlation times.

The dynamical behavior of solid C_{60} parallels that of the classic solid-state rotator adamantane (*25*). Adamantane also undergoes a phase transition, from tetragonal to orientationally disordered FCC at 213 K (*26*). Rotational correlation times for both phases have been measured and fit to Arrhenius expressions. The high-temperature disordered (α) phase has an activation energy $E_a^{\alpha} = 3.1$ kcal mol^{-1} (about twice E_a^{Rot}) and $\tau_0^{\alpha} = 9 \times 10^{-14}$ s. At 283 K, for example, $\tau^{\alpha} = 22$ ps, giving a value of $\chi \approx 30$. The corresponding χ for C_{60} is one-tenth of that. In the low-temperature ordered (β) phase, τ increases by a factor of ~40, and the Arrhenius parameters are $\tau_0^{\beta} = 1 \times 10^{-15}$ s and $E_a^{\beta} = 6.5$ kcal mol^{-1}. At 200 K, $\tau^{\beta} = 13$ ns, 4.5 times as long as τ for C_{60} (2.9 ns at 200 K). The similar behavior of these two substances suggests that (i) the orientationally ordered

phases of both molecules have rotational potentials with fairly deep minima and (ii) above the phase transition, random orientations of neighboring molecules lead to a much smoother potential, with numerous shallow potential minima. For the rotator phase of C_{60} the extraordinary smoothness of this potential results in a rate of molecular reorientation that approaches the gas-phase rate and exceeds the value found for C_{60} in solution.

REFERENCES AND NOTES

1. C. S. Yannoni, R. D. Johnson, G. Meijer, D. S. Bethune, J. R. Salem, *J. Phys. Chem.* **95**, 9 (1991).
2. R. Tycko *et al.*, *ibid.*, p. 518.
3. P. A. Heiney *et al.*, *Phys. Rev. Lett.* **66**, 2911 (1991).
4. R. Tycko *et al.*, *ibid.*, p. 1886.
5. W. Krätschmer *et al.*, *Nature* **347**, 354 (1990).
6. R. D. Johnson, G. Meijer, J. R. Salem, D. S. Bethune, *J. Am. Chem. Soc.* **113**, 3619 (1991).
7. F. Diederich *et al.*, *Science* **252**, 548 (1991).
8. R. Freeman, in *Dynamic Nuclear Magnetic Resonance Spectroscopy*, L. M. Jackson and F. A. Cotton, Eds. (Academic Press, New York, 1975).
9. H. W. Spiess, in *NMR: Basic Principles and Progress*, P. Diehl, E. Fluck, R. Kosfeld, Eds. (Springer-Verlag, Berlin, 1978), vol. 15, p. 55.
10. F. A. L. Anet, D. J. O'Leary, C. G. Wade, R. D. Johnson, *Chem. Phys. Lett.* **171**, 401 (1990).
11. For isotropic diffusional reorientation the autocorrelation function for a tensor function of rank l of the angular coordinates decays with a time constant given by $1/l(l + 1)D$, where D is the rotational diffusion constant and τ_A and τ_S are associated with $l = 1$ and 2, respectively. See (*9*) for details.
12. P. P. Bernier *et al.*, paper presented at the Experimental NMR Conference, St. Louis, MO, 7 to 11 April 1991.
13. $S^2 = \Delta\sigma^2(1 + \eta^2/3)$, with $\Delta\sigma \equiv \sigma_{33} - (\sigma_{22} + \sigma_{11})/2$ and $\eta \equiv (\sigma_{22} - \sigma_{11})/(2\Delta\sigma/3)$. See (*9*) for details.
14. J. C. Facelli, A. M. Orendt, D. M. Grant, J. Michl, *Chem. Phys. Lett.* **112**, 147 (1984).
15. R. D. Johnson *et al.*, in preparation.
16. C. S. Yannoni *et al.*, *J. Am. Chem. Soc.* **113**, 3190 (1991).
17. K. Hedberg *et al.*, *Science* **254**, 410 (1991).
18. S. Liu *et al.*, *ibid.*, p. 408.
19. W. I. F. David *et al.*, *Nature* **353**, 147 (1991).
20. R. T. Boere and R. G. Kidd, *Annu. Rep. NMR Spectrosc.* **13**, 319 (1982).
21. W. B. Moniz, W. A. Steele, J. A. Dixon, *J. Chem. Phys.* **38**, 2418 (1963).
22. D. A. Neumann *et al.*, *Phys. Rev. Lett.*, in press.
23. A. Cheng and M. L. Klein, *J. Chem. Phys.* **95**, 6750 (1991).
24. F. Reif, *Statistical Physics* (McGraw-Hill, New York, 1975).
25. H. A. Reiley, *Mol. Cryst. Liq. Cryst.* **101**, 9 (1969).
26. C. E. Nordmann and D. L. Schmitkons, *Acta Crystallogr.* **18**, 764 (1965).

27. We acknowledge the help of L. Taylor and P. Jedrzejewski in preparing the sample, the technical assistance of G. May, and stimulating conversations with R. Tycko and F. A. L. Anet.

26 September 1991; accepted 18 November 1991

Diffusion Creep in Perovskite: Implications for the Rheology of the Lower Mantle

SHUN-ICHIRO KARATO AND PING LI

High-temperature creep experiments on polycrystalline perovskite ($CaTiO_3$), an analog of (Mg,Fe)SiO_3 perovskite of the lower mantle, suggest that (grain size–sensitive) diffusion creep is important in the lower mantle and show that creep rate is enhanced by the transformation from the orthorhombic to the tetragonal structure. These observations suggest that grain-size reduction after a subducting slab passes through the 670-kilometer discontinuity or after a phase transformation from orthorhombic to tetragonal in perovskite will result in rheological softening in the top portions of the lower mantle.

DYNAMICS OF EARTH'S INTERIOR depend critically on the plastic flow properties of its constituent materials. Plastic flow in rocks occurs either by the collective motion of atoms by dislocation glide (or climb) or by the diffusive transport of individual atoms. The constitutive relation for creep between the two mechanisms is quite different, and this difference can significantly influence the dynamics of Earth's interior (*1*). Creep rate by dislocation motion is insensitive to grain size and increases nonlinearly with stress, whereas creep rate due to diffusion increases dramatically as grain size decreases and increases linearly with stress. Recent studies on crustal and upper mantle minerals show that the transition conditions between the two mechanisms are close to the conditions expected in Earth's crust and the upper mantle (*2*). Thus diffusion creep is a distinct possibility in Earth and might be a dominant mechanism of flow when a significant reduction in grain size occurs. Such a grain-size reduction is expected when a subducting slab passes through the phase transformation boundaries (*3*). For example, Ito and Sato (*4*) showed a significant grain-size reduction after the transformation of $(Mg,Fe)_2SiO_4$ into (Mg,Fe)SiO_3 perovskite + (Mg,Fe)O magnesiowustite (at 23 GPa or ~670 km) and suggested that rheological softening might occur if grain-size reduction occurs under differential stress. However, experimental data are lacking to examine the possibility of diffusion creep in perovskite, the mineral that makes up most of the lower mantle (670 to 2900 km).

In this study, we investigated the creep law of perovskite in the grain size–sensitive regime using $CaTiO_3$ as an analog material. Dislocation creep behavior has been studied in single crystals of analog materials of (Mg,Fe)SiO_3 perovskites (*5*), but understanding the process of deformation of polycrystalline aggregates is important because grain size–sensitive diffusion creep occurs only in polycrystalline specimens. $CaTiO_3$ perovskite is a good analog material of (Mg,Fe)SiO_3 perovskite for two reasons. First, the crystal structures are similar: both belong to the same space group *Pbnm* at ambient temperature (and pressure) (*6*) and transform to higher symmetry structures at higher temperatures (*7*). In addition, there are similarities in defect structures: the same slip systems of dislocations have been identified in both types of perovskites (*5, 8*), and the same types of point defects occur in both perovskites (*9*). A particularly attractive aspect of $CaTiO_3$ behavior is that structural phase transformations occur at high homologous temperatures ($T/T_m > 0.68$, where T_m is the melting temperature), where the material shows significant plastic flow.

We prepared dense fine-grained (5 to 27 μm) aggregates of $CaTiO_3$ perovskite by hot-pressing commercially available powder specimens. In the hot-pressing, we used a gas-medium apparatus in an iron jacket at 300 MPa and 1200°C for 1 to 2 hours. The hot-pressed specimens have densities that are better than 96% of theoretical values and uniform grain-size distributions (Fig. 1) (*10*). Transmission electron microscopy observations indicated no precipitation and no secondary phases at grain boundaries at a resolution of ~5 nm. The hot-pressed specimens were cut in a parallelepiped shape (~3 by 3 by 6 mm^3) and were deformed in

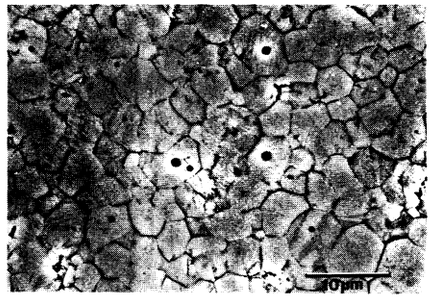

Fig. 1. A scanning electron micrograph of hot-pressed $CaTiO_3$ perovskite after etching. Note the homogeneous grain size and equilibrium grain boundaries.

Department of Geology and Geophysics, University of Minnesota, Minneapolis, MN 55455.